

Optical absorption of small copper clusters in neon: Cu_n , ($n = 1-9$)

S. Lecoultré,¹ A. Rydlo,¹ C. Félix,² J. Buttet,¹ S. Gilb,³ and W. Harbich^{1,a)}

¹*Institut de Physique de la Matière Condensée, École Polytechnique Fédérale de Lausanne, 1015 Lausanne, Switzerland*

²*Meteo Swiss, 1530 Payerne, Switzerland*

³*MS-ROK Research Informatics, Merck KGaA Frankfurter Str. 250, 64293 Darmstadt, Germany*

(Received 12 October 2010; accepted 14 January 2011; published online 15 February 2011)

We present optical absorption spectra in the UV-visible range ($1.6 \text{ eV} < \hbar\omega < 5.5 \text{ eV}$) of mass selected neutral copper clusters Cu_n ($n = 1-9$) embedded in a solid neon matrix at 7 K. The atom and the dimer have already been measured in neon matrices, while the absorption spectra for sizes between Cu_3 and Cu_9 are entirely ($n = 6-9$) or in great part new. They show a higher complexity and a larger number of transitions distributed over the whole energy range compared to similar sizes of silver clusters. The experimental spectra are compared to the time dependent density functional theory (TD-DFT) implemented in the TURBOMOLE package. The analysis indicates that for energies larger than 3 eV the transitions are mainly issued from d-type states; however, the TD-DFT scheme does not reproduce well the detailed structure of the absorption spectra. Below 3 eV the agreement for transitions issued from s-type states is better. © 2011 American Institute of Physics. [doi:10.1063/1.3552077]

I. INTRODUCTION

The size dependent evolution of the structural, physical, and chemical properties of finite size aggregates has been the subject of numerous basic and applied researches. Since the beginning optical spectroscopy has been a powerful technique to study the electronic properties of clusters and their structural properties by comparison with the calculated optical spectra.^{1,2}

From a fundamental point of view, clusters of noble metal elements are of particular interest, since they form a bridge between simple and transition metal clusters and allow to study the influence of the d electrons on the optical properties. It is, for example, well known that the d contributions strongly influence the optical response of the surface plasmon in large noble metal particles.³ While silver develops a strong and narrow plasmon absorption centered at 4 eV, followed by interband transitions at higher energies, the surface plasmon in copper is strongly damped by s-d hybridization effects and interband transitions.^{3,4} The concentration of oscillator strength (OS) in the energy range of the surface plasmon in silver is visible down to the smallest cluster sizes,⁵ and explains why the experimental study of the optical absorption of neutral noble metal clusters beyond the trimer was limited to Ag clusters, which have, in the UV-visible range, a cross section considerably larger than that of gold or copper clusters.⁶

Measurements on free mass selected species are limited by the low density of particles. We have thus undertaken since several years⁷ to condense mass selected clusters in rare gas matrices in order to study their optical properties. Recent improvements in the experimental sensitivity⁸ and the use of low

temperature neon matrices make the copper and gold clusters⁶ accessible to experiment. We present in this paper the absorption spectra that were obtained for neutral Cu_n ($n = 1-9$) clusters condensed in a neon matrix at 7 K. The atom and the dimer have already been measured in neon matrices^{9,10} together with their fluorescence spectra, and in other rare gas matrices.¹¹⁻¹⁴ Some results up to Cu_5 have been published from studies in argon, xenon, or CH_4 matrices;^{11,13} however, these measurements were achieved using photoaggregation and thermoclustering techniques, starting from the atom. In these techniques, the attribution of absorption lines to a specific size is a difficult task since the spectra are filled up with the absorption of lower size clusters and, even more important, the structure of the cluster is rather determined by diffusion aggregation, which is not necessarily the ground state of the copper cluster. Mass selection prior to deposition is a convenient way to circumvent these difficulties.

Our measurements are compared to the time dependent density functional theory (TD-DFT) calculations with the b3-lyp functional, which is also suitable for the other coinage metal clusters and gives excellent agreement between experiment and theory for Ag. No previous absorption TD-DFT spectra of copper clusters have been published to our knowledge, although detailed studies are known for Ag (Refs. 15-17) and Au (Refs. 18 and 19) clusters.

II. EXPERIMENTAL

As mentioned in the Introduction, we report in the present work measurements of the UV-visible absorption of copper clusters deposited in a neon matrix at 7 K. Clusters are formed from a metal target sputtered by a 10 mA Xe^+ ion beam at 25 keV. The copper cations are then focused into a “Bessel Box” type energy filter which also acts as a beam stop for the intense flux of neutrals. The cations of interest are mass

^{a)}Electronic mail: wolfgang.harbich@epfl.ch.

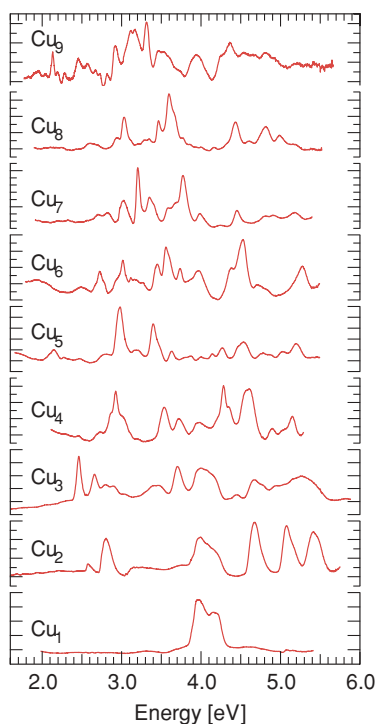


FIG. 1. Experimental absorption spectra of Cu_n , $n = 1-9$ obtained in a neon matrix at 7 K.

selected and directed toward the sample holder, which consists in a superpolished aluminum mirror (Valley Design Corp.). The sample holder is fixed to a cold head cryostat (SRP-052A Cryocooler, Sumitomo Heavy Industries Ltd.) that allows refrigeration to 7 K. Size selected clusters are codeposited with Ne at a dilution $D \leq 3 \times 10^5$ at a total kinetic energy below 20 eV. This value is a good compromise between fragmentation and signal intensity.²⁰ The total matrix thickness equals 50 μm .

Optical absorption measurements are performed by injecting light through the 2 mm length of the matrix and collecting the transmitted light on the other side by an optical fiber of 400 μm core diameter. The collected light is analyzed by an optical spectrometer coupled to a liquid-nitrogen-cooled charge coupled device (CCD). Comparing the light intensity passing through a matrix doped with clusters with a reference signal of light passing through a pure neon matrix yields the absorption spectrum. Typical numbers of deposited charges inside the matrix are comprised between 8 nAh for the atom and 450 pAh for the hexamer, corresponding, respectively, to cluster densities of $3.6 \times 10^{15} \text{ mm}^{-3}$, dilution of $1 : 3 \times 10^5$ and $2 \times 10^{14} \text{ mm}^{-3}$, dilution of $1 : 5 \times 10^6$.

III. COMPUTATION

Numerous calculations have studied the lowest energy structures of copper aggregates using different calculation schemes. For a comprehensive review, we refer the reader to the recent paper by Yang *et al.*²¹ and references therein. Our results for the lowest energy isomers (see Fig. 2) are in close agreement with those obtained recently within the DFT formalism. Some calculations of the excited states of neutral

copper clusters have been done, they are however limited to dimers and trimers.²²⁻²⁴

In the present study, the TD-DFT was used to describe the electronic structure and the UV-visible absorption spectra of Cu_n ($n = 1-9$). A calculation scheme was used, which is also suitable for the other coinage metals. The b3-lyp (Refs. 25 and 26) functional together with the def2-TZVP basis ([17s11p7d1f]/[6s4p4d1f]) as implemented in the TURBOMOLE package was chosen.²⁷ In order to check for consistency and to compare to results found in the literature, for a few cluster sizes the calculations of the different ground state geometries and their relative energies were repeated with the Perdew-Becke-Ernzerhof functional. The different functionals did not lead to any significant difference in the results. All electrons (28 per atom) were treated fully in the calculation. Quadrature grids were of m3 quality.²⁸ The geometry optimization was started using structures found in the literature and at least the two lowest lying isomers from calculations by Fernández *et al.*²⁹ were evaluated. The geometry optimizations are carried out with symmetry restriction when applicable. A normal mode analysis was applied to each stationary geometry to ensure local minima. The TD-DFT calculations were performed with the ESCF module³⁰ of the TURBOMOLE V-5.9 program package.³¹

IV. RESULTS

The as observed experimental absorption spectra of small neutral copper clusters Cu_n ($n = 1-9$) deposited and neutralized after mass selection in a neon matrix at 7 K are given in Fig. 1. As clearly visible from the Cu_1 - Cu_3 spectra, fragmentation is present. The systematic measurement of successive sizes allows to eliminate the fragmentation products. The lower trace of Fig. 2 (red curve) presents the “cleaned” experimental spectra. They have been obtained by deconvoluting the measured spectra in a sum of Gaussians, whose positions correspond to the measured peaks, while their line width and amplitude were determined by a least square fit. The obtained line widths are typically comprised between 50 and 150 meV. The absorption lines attributed to fragmentation into Cu_1 and Cu_{n-1} have been subtracted in order to obtain the absorption traces for given size clusters.

Table I gives the peak position and integrated cross section of the different transitions observed. The cross section was determined by integrating the corresponding absorption line normalized to the cluster density. We estimate the absolute error to be of the order of 50%, while the relative error from one transition to the other for one cluster size is considerably smaller.

The TD-DFT spectra of the two lowest lying Cu isomers obtained in the calculation scheme described above are given in Fig. 2 (upper black traces). We have made a Mulliken population analysis of the states involved in the transitions in order to determine the principal s, p, or d contributions of the Kohn-Sham molecular orbitals involved in a given transition. The absorption lines whose initial state is predominantly of s-type, have been noted by a black dot, and we shall speak of s-s or s-p transitions depending on the principal s or p character of the final state. The remaining absorption lines,

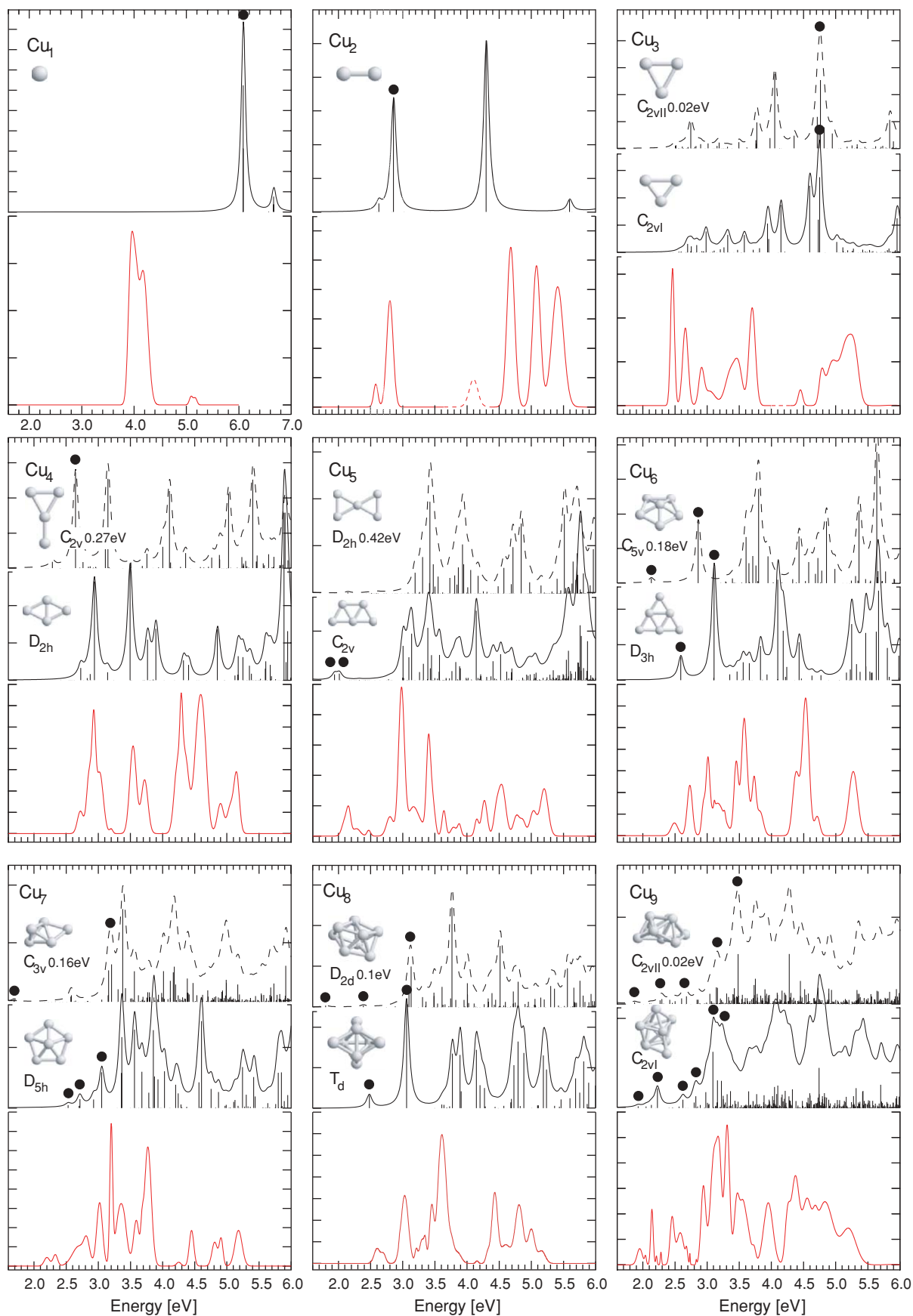


FIG. 2. Comparison between experimental and calculated absorption spectra for copper clusters. Experimental “cleaned” absorption (see text)—lower curve. The TD-DFT calculations for the ground state configuration—continuous black line—and next higher isomer—interrupted black line. The transitions have been broadened by Lorentzians of 0.1 eV FWHM. The black dot identifies transitions whose initial state is predominantly of s type. The vertical scale for the TD-DFT calculation is a measure of the oscillator strength per atom, one interval corresponding to 0.025 units.

TABLE I. Peak positions in eV and integral of the cross-section over the energy of the corresponding transition. The oscillator strength is obtained by multiplying the integrated cross section (in $10^{-18} \text{ cm}^2 \text{ eV}$) by $1.12 \cdot 10^{-2}$.

Species	Peak position (integrated cross-section) [eV] ($[10^{-18} \text{ cm}^2 \text{ eV}]$)
Cu ₁	3.94(7.03), 4.03(5.27), 4.14(4.89), 4.22(5.57), 5.09 (0.28), 5.17 (0.21)
Cu ₂	2.58(0.48), 2.80(3.37), 4.68(5.89), 5.08(5.28), 5.41(6.77)
Cu ₃	2.46(6.30), 2.66(5.25), 2.91(2.17), 3.04(1.91), 3.37(4.70), 3.49(2.93), 3.70(7.62), 4.45(0.86), 4.78(1.81), 4.94(5.71), 5.17(9.31), 5.30(3.78),
Cu ₄	2.72(2.05), 2.86(5.01), 2.93(5.16), 3.02(6.90), 3.20(0.22), 3.54(9.07), 3.72(5.49), 4.23(6.91), 4.29(2.84), 4.35(8.46), 4.57(17.40), 4.65(4.66), 4.90(2.97), 5.05(2.35), 5.15(5.14)
Cu ₅	2.10(0.96), 2.16(0.97), 2.28(0.58), 2.47(0.22), 2.80(1.42), 2.98(8.96), 3.15(1.47), 3.22(2.43), 3.40(3.94), 3.47(1.66), 3.64(1.04), 3.79(0.52), 3.88(0.43), 4.15(0.69), 4.27(2.05), 4.45(0.87), 4.54(4.13), 4.77(1.33), 4.87(0.79), 5.03(1.76), 5.20(3.85)
Cu ₆	2.49(1.92), 2.67(0.22), 2.73(5.57), 2.94(2.11), 3.01(5.41), 3.11(0.18), 3.16(9.77), 3.27(0.24), 3.45(6.98), 3.57(9.32), 3.61(7.26), 3.73(3.97), 3.82(3.44), 4.38(8.95), 4.53(20.37), 4.71(2.19), 5.27(12.54)
Cu ₇	2.20(1.18), 2.33(1.30), 2.70(6.67), 2.82(2.73), 3.02(9.19), 3.20(9.41), 3.35(14.68), 3.41(0.05), 3.59(6.17), 3.68(1.58), 3.77(20.39), 4.25(0.04), 4.45(4.03), 4.81(3.26), 4.91(2.50), 5.18(6.49)
Cu ₈	2.60(1.47), 2.70(0.07), 3.03(8.38), 3.21(0.59), 3.30(2.02), 3.35(0.61), 3.45(4.15), 3.58(8.93), 3.65(8.64), 3.76(1.30), 3.85(1.39), 4.16(0.12), 4.32(0.63), 4.43(6.67), 4.60(2.96), 4.81(7.74), 5.00(3.69), 5.16(1.53)
Cu ₉	1.95(0.03), 2.14(0.04), 2.45(0.06), 2.58(0.07), 2.68(0.01), 2.94(1.10), 3.11(2.60), 3.19(1.05), 3.31(2.10), 3.46(1.04), 3.55(0.09), 3.63(0.06), 3.73(0.02), 3.95(1.74), 4.25(0.07), 4.37(2.07), 4.55(1.65), 4.68(0.02), 4.83(3.10), 5.21(1.59)

issued predominantly of the d band, correspond to d-s or d-p transitions.

A. Absorption spectra and fragmentation

The deconvolution of the absorption spectra, as described above, yields the content of fragments inside the matrix. We find, as expected, decreasing fragmentation rates going from the dimer to the nonamer.

In the spectrum of the dimer (Fig. 1), the atomic structure is visible between 3.85 and 4.3 eV. Extracting the atomic transitions reveals an additional Cu₂ peak hidden by the presence of the atom. This transition is added as a dotted line centered around 4.1 eV in Fig. 2. The apparently negative absorption band at 3.05 eV is due to the dimer fluorescence captured by the optical fiber. The fluorescence of the atom is also visible at 3.56 eV.

In the trimer case, the atom signal is also clearly visible, and like in the case of the dimer, one cannot exclude that an additional Cu₃ peak is hidden by the atom (see the dot-

ted line). Since the fragmentation of Cu₃ proceeds into one monomer and one dimer, we expect and indeed observe the spectroscopic fingerprint of Cu₁ and Cu₂

The atom signal is also visible in the tetramer spectrum at 3.99 eV, the small signal at 2.46 eV is attributed to the trimer resulting from the fragmentation of Cu₄ in Cu₃ and Cu atom. For the pentamer no fragmentation is observable, except may be the discrete presence of the atom at 4.00 eV, which has been suppressed in the “cleaned” experimental spectrum. In the Cu₆ spectrum, the monomer is probably present at 3.98 eV, and it is not excluded that a small contribution coming from the pentamer adds to the hexamer peaks at 3.01, 3.45, and 4.53 eV. For the heptamer, one can exclude the presence of fragmentation, as no Cu₆ transition is visible. Notice, however, that a small peak at 3.98 eV is still present indicating the presence of the atom. For the octamer or the nonamer there is no clear sign of fragmentation.

Notice that all absorption spectra up to $n = 7$ reveal the presence of copper atoms inside the neon matrix, while there is no Cu _{$n-1$} signal in a corresponding proportion. This suggests that not only fragmentation upon impact is responsible for the presence of Cu atoms in the spectra, but also evaporative cooling from the sputtered clusters. It is known that the hot clusters produced via a sputtering process cool down by evaporation of atoms.³² If this evaporation takes place after the Bessel Box, neutral atoms can contaminate the neon matrix since the ratio between the initial clusters velocity and the drift velocity after dissociation is small. By comparing our values to the experiments on evaporative cooling from clusters formed by sputtering,³² we find that this phenomenon is very likely to happen in our case, explaining the observed atom signal.

B. Comparison with known experimental results and TD-DFT calculations

In what follows we shall examine size by size the experimental absorption spectra, and compare them with known results when available, i.e., essentially up to the tetramer. As already mentioned the absorption spectra for sizes comprised between Cu₆ and Cu₉ are entirely new. We shall also compare size by size the predictions of the theory with the experimental data.

Before starting any detailed analysis, the first observation to make is the large amount of transitions and the complexity of the spectra. This is particularly relevant if we compare them to the absorption spectra in silver clusters.^{16,33} We shall discuss later these differences, closely related to the importance of the s-d hybridization and d contributions for the Cu clusters.

Cu₁: The experimental spectrum of Cu₁ presented in Fig. 2 is composed of a wide structure between 3.85 and 4.30 eV and a smaller intensity double peak structure at 5.09 and 5.17 eV. The main absorption feature is not well enough resolved in order to find the exact position of the underlying absorption lines. It can be decomposed in four lines of similar intensities as shown in Table I.

Our measurements are in excellent agreement with synchrotron radiation measurements performed in a neon matrix

by Kolb *et al.*,⁹ who also observe a band situated between 3.9 and 4.1 eV and a small intensity double peak structure at 5.13 and 5.16 eV at the low energy side of a band comprised between 5.1 and 6.2 eV. The broad structure around 4.0 eV is attributed to the 4s-4p transitions ${}^2P_{1/2,3/2} \leftarrow {}^2S_{1/2}$ while the two peaks around 5.1 eV are attributed to the 3d-4p absorption ${}^4P_{3/2} \leftarrow {}^2S_{1/2}$ split by crystal field effects. Notice that in the other rare gas matrices^{12–14} the 4.0 eV structure is clearly formed of three different peaks corresponding to the ${}^2P_{1/2,3/2} \leftarrow {}^2S_{1/2}$ transitions split by Jahn–Teller and crystal field effects. It has been suggested that the substitutional site in neon is too small to accommodate the Cu atom, and a larger and less well ordered trapping site is created, explaining the broad and nonresolved structure observed in neon. In the gas phase the s–p transitions are measured at 3.79 and 3.82 eV (Ref. 34) and the 3d–4p transition at 4.97 eV. They are in good agreement with the average values of the absorption lines observed in matrices if we include a blue shift of 0.2 eV.

Our TD-DFT calculation (see Fig. 2) was unable to reproduce the experimental data, instead it gives two peaks at 6.0 and 6.3 eV mainly issued from, respectively, the 4s and 3d atomic states. Notice that in the case of the silver atom, a TD-DFT calculation made within the same scheme³³ reproduces better the experimental results, it gives a 4s–4p transition situated at 4.02 eV, while the average gas phase value is equal to 3.74 eV. The difference is related to the relatively large s–d gap in silver compared to copper. Notice also that in silver the inner electrons were described by an electron core potential, while in the copper calculation all electrons are taken into account.

Cu₂: The measured spectrum of the copper dimer is composed of five well-defined peaks at 2.58, 2.80, 4.68, 5.08, and 5.41 eV. A further transition is found at 4.1 eV. This peak is hidden by the principal transition of Cu₁. We have extracted this peak which is given as a dotted line in Fig. 2 by subtracting the monomer from the dimer spectrum. Because of a remaining uncertainty, this transition is not reported in Table I. The influence on the measured cross section for Cu₂, however, is small.

Among all metal dimers, Cu₂ is one of the most studied systems in literature. In particular, absorption in neon has already been measured by Kolb *et al.*,⁹ who have been able to discriminate between the Cu atom and the dimer absorption spectra by recording their emission yield spectra. They obtain for the dimer a weak absorption peak at 2.64 eV, larger intensity peaks at 2.85 and 4.2 eV, and three main structures formed of several peaks situated between 4.64–4.80, 5.02–5.17, and 5.34–5.41 eV, as well as other peaks at energies beyond the range of our measurements. Our data are in excellent agreement with these measurements if we also include in our measured spectrum the absorption peak at 4.1 eV hidden by the presence of the Cu atoms (given in dotted red line in Fig. 2). Other measurements in argon, krypton, and xenon matrices^{11–13} show several transitions between 3 and 3.5 eV that are not observed in neon. The gas phase absorption spectrum of Cu₂ (Ref. 35) is dominated by transitions into two low lying electronic states, denoted A and B, and situated, respectively, at 2.53 and 2.70 eV. They correspond well to our data for the peaks measured at 2.58 and 2.80 eV.

Kolb *et al.*⁹ have discussed the dimer absorption and emission bands on the basis of the theoretical calculations of Miyoshi *et al.*²⁴ and have derived an energy level scheme compatible with their measurements. More recent DFT calculations²² have studied the spectroscopic properties of Cu, Ag, and Au dimers, and assigned the measured gas phase spectroscopic terms to given transitions. They find, in particular, for copper that the B state corresponds to a transition from the singlet ground state to a singlet excited state (${}^1\Sigma_u^+$) formed by promotion of an electron from the predominantly s-type HOMO bonding state to the antibonding LUMO state. They also assign the A state to an electronic transition from d to s-type orbitals, whose oscillator strength is weaker than that of the B state.

Comparison with the TD-DFT calculation gives a good agreement for the three peaks at low energies, the three intense peaks above 4.5 eV are, however, not reproduced. Our calculation indicates that the large intensity transition at 2.85 eV corresponds to the B state. It results like in Wang's calculation from the promotion of an electron from the HOMO predominantly s state to the antibonding LUMO state. The agreement between its measured (2.58 eV) and calculated (2.62 eV) position suggests that the low energy peak corresponds to the A excited state. Indeed we find, as predicted by Wang, that it is a d–s type transition. Notice also that the calculated transition at 4.3 eV is related to promotion of a d electron to the mainly s-type LUMO orbital. The calculated Ag₂ absorption is also formed of two intense absorption lines at energies comparable to that of Cu₂; however, they are both issued from the HOMO s state, and are principally of s–s and s–p type.^{15,17} Notice that the degree of s–d hybridization in Ag is smaller than in copper.

Cu₃: The Cu₃ spectrum is formed of a large number of transitions starting abruptly with an intense and narrow line at 2.46 eV. Other well-defined peaks are visible at 2.66, 2.91, 3.04, 3.70, 4.45, 4.78, and 4.94 eV. Larger structures, formed of at least two peaks are centered around 3.45 and 5.2 eV.

The copper trimer is among the most thoroughly investigated of any metal cluster species, and several studies^{36–38} have debated to know if Cu₃ possesses a well-defined bent structure or is fluxional in a matrix environment. The first identification of Cu₃ was reported in matrices of methane and argon¹¹ by Moskovits and Hulse, who found six absorption peaks in the UV-visible range starting on at 2.48 eV. Measurements in xenon¹³ using photoaggregation techniques have reported two absorption lines at 2.60 and 4.54 eV, as well as a new line at 2.84 eV resulting from interconversion induced by photolysis between the acute and obtuse C_{2v} geometries. Detailed gas phase spectroscopic studies of Cu₃ have been reported.^{39–41} In particular, Knickelbein⁴¹ measured the photodissociation spectra of Cu₃, Cu₃Ar, and Cu₃Kr. They observe in the gas phase for the bare copper trimer a vibrationally resolved band whose origin is at 2.30 eV (maximum around 2.35 eV) and a broad continuous band with a maximum near 2.56 eV. These bands are assigned to the A ← X and B ← X transitions calculated at, respectively, 2.14 and 2.42 eV in the SCF/C study of Walch and Laskowski.²³ Notice that for Cu₃ Ar the corresponding maxima of the A ← X and B ← X transitions are measured, respectively, at

2.40 and 2.51 eV, with a large increase of the $A \leftarrow X$ transition oscillator strength. Knickelbein suggests that the absorption line measured at 2.48 eV by Moskovits and Hulse¹¹ in an argon matrix corresponds to the $A \leftarrow X$ transition measured at 2.35 eV in the gas phase and that the lower intensity $B \leftarrow X$ transition could not be observed in their measurements. Following these lines we suggest that the lower energy peak measured at 2.46 eV in our measurements corresponds also to the $A \leftarrow X$ transition, it is also plausible that the 2.66 eV peak corresponds to the $B \leftarrow X$ transition.

All published calculations^{23,24,42} indicate that the Jahn–Teller effect gives rise to obtuse and acute C_{2v} structures, very close in energy. The most recent calculations performed in the framework of DFT (Refs. 29, 43–47) predict the obtuse geometry as the ground state. This is also the case in the present work, the two geometries are, however, separated by only 0.02 eV. The TD-DFT spectra for both isomers are given in Fig. 2. The agreement between theory and experiment is certainly not good, in particular, the high intensity transitions at low energy are not reproduced. The analysis indicates for both structures that all transitions, except one, up to 5 eV are of d–s type, while the transitions above 5 eV are of d–p type. The weak intensity around 5.5 eV corresponds to the energy range where the nature of transitions evolves from a d–s to a d–p type. It is interesting to notice that the general shape of the linear trimer absorption is in better agreement with the experiment. In particular, the strong transition measured at 2.46 eV corresponds well to the main s-type peak calculated at 2.67 eV.

Cu₄: The spectrum of the copper tetramer is composed of well-defined peaks at 2.93, 3.54, 3.72, 4.29, 4.57, 4.90, and 5.15 eV. Smaller intensity transitions and shoulders are visible at 2.72, 2.86, 3.02, 3.20, 4.35, and 5.05 eV. The spectral resolution allows to see peaks as narrow as 100 meV at 2.93 and 4.29 eV for example.

Previous measurements of Cu₄ have been achieved in argon and CH₄ matrices by warming samples containing a high density of copper atoms. One intense peak at 3.08 eV in argon and two peaks at 2.92 and 4.56 eV in CH₄ have been reported.¹¹ Cu₄ was also reported in xenon by photoaggregation and thermoclustering techniques.¹³ Absorption lines are reported at 2.26, 2.33, 2.41, 2.95, and 4.71 eV and attributed to the presence of two distinct site isomers. Comparison of these results with our data suggests that the peak obtained at 3.08 eV in argon, 2.92 eV in CH₄, and 2.95 eV in xenon correspond to the strong absorption peak reported in our measurements at 2.93 eV.

Several calculations addressed the low energy configurations of Cu₄ using SCF (Refs. 48 and 49) or DFT (Refs. 29, 43–46, 50–53) schemes. All recent calculations agree that the planar D_{2h} geometry corresponds to the ground state structure. Like in the case of Cu₃ the Mulliken population analysis indicates (for the rhombus structure) that the transitions up to 5 eV are of d–s type, while they are of the d–p type for higher energies. There is, however, a sizeable contribution of the HOMO s state to the d–s transitions. The experimental spectrum is clearly the sum of a large number of transitions, reflecting the numerous d–s and d–p transitions contributing to the calculated absorption. Notice that for the

D_{2h} structure the major peaks observed at low energy can be correlated to the main calculated ones, suggesting that the absorption spectrum corresponds to the rhombus.

Cu₅: Cu₅ is characterized by two strong transitions at 2.98 and 3.40 eV and a large number of smaller ones. Notice in particular the double structure at 2.10 and 2.16 eV situated at the low energy side of the absorption spectrum. Using a very high Cu/Xe ratio of 1%, Ozin *et al.*¹³ were able to obtain absorption peaks by photoaggregation techniques tentatively assigned to Cu₅ at 2.12, 4.11, and 4.48 eV. These results are not confirmed by our measurements, they do not mention in particular the large intensity transitions at 2.98 and 3.40 eV. The low energy structure around 2.1 eV could, however, correspond to the 2.12 eV absorption peak mentioned by Ozin.

All SCF (Ref. 49) and DFT calculations,^{29,44–46,50,52,53} including ours, confirm the C_{2v} isomer as the most stable geometry. The Mulliken population analysis for the C_{2v} geometry indicates also that there are two groups of transitions, they are of d–s type between 2.5 and 5 eV and of d–p type above 5 eV. The two small intensity transitions around 2 eV, issued from the HOMO-1 and HOMO-2 orbitals, are however mainly of s–s type, suggesting that the two transitions observed around 2.2 eV also correspond to s-type transitions. This is an indication, together with the relatively good agreement between theory and experiment in the range 2.5–3.5 eV, that the observed clusters are of C_{2v} symmetry. It is worthwhile to notice that the experimental spectrum of Ag₅ resembles closely that of Cu₅, if we only take into account the two larger intensity structures. However, the TD-DFT calculation^{16,33} indicates that they are issued in Ag from s-type states and not from d-type states.

Cu₆: Several intense transitions are visible at 2.49, 2.73, 3.01, 3.45, 3.57, 3.73, 4.53, and 5.27 eV as well as smaller ones given in Table I. No previous absorption spectrum has been reported for the neutral cluster.

Different DFT calculations were performed on this system,^{29,43,44,46,51–53} all of them including ours find the planar D_{3h} structure to be the most stable isomer, in close competition with the C_{5v} and C_{2v} three-dimensional structures. The analysis indicates, such as in the case of Cu₅, that the low energy transitions, typically below 3 eV, are issued of the predominantly s-type HOMO Kohn–Sham orbital, while they are of d–s type between 3 and 5 eV and of d–p type above 5 eV. Within a small shift of 0.1 eV the calculated low energy transitions reproduce well the experimental peaks if we admit the coexistence of both the D_{3h} and C_{5v} isomers in the sample. In particular the strong s–s transition at 3.1 eV for the D_{3h} structure and 2.85 eV for the C_{5v} geometry correspond to the narrow transitions measured, respectively, at 3.01 and 2.73 eV.

Cu₇: The spectrum of Cu₇ is characterized by intense transitions at 3.20 and 3.77 eV and well resolved smaller intensity structures. Our DFT calculation, as well as recent calculations,^{29,44,46,52,53} find that the ground state configuration is the three-dimensional D_{5h} structure, lying just below the C_{3v} structure. The low energy part of the spectrum, of s–s type, corresponds well with the calculation for the D_{5h} structure if we include a shift of ~ 0.2 eV. This is an indication, together with the similarity of the general behavior of the

theoretical and calculated spectra, that our sample contains mainly clusters with a D_{5h} geometrical structure.

Cu_8 : The experimental spectrum of the octamer shows well-defined peaks at 3.03, 3.45, 3.59, 4.43, 4.81 eV, and smaller intensity structures. We find in agreement with previous DFT calculations^{21,29,43,44,46,52,53} that the T_d and D_{2d} geometries are close in energy. Cu_8 is a special case since in the jellium model it corresponds to a closed shell cluster. For the T_d geometrical configuration, we find a strong intensity transition at 3.06 eV, which initiates from the HOMO predominantly s state. For the D_{2d} structure the intense transition at 3.12 eV is issued from the HOMO and HOMO-1 s state, with a larger d contribution. Both transitions correspond well to the peak observed at 3.03 eV. Notice however that the experimental spectrum shows a closer resemblance with the calculated one for the D_{2d} structure. Notice also that the double peak structure of the absorption around 2.6 eV suggests, such as in the case of Ag_8 ,¹⁶ that both isomers contribute to the absorption.

Cu_9 : The spectrum of Cu_9 shows a large amount of sharp transitions over the whole energy range. It was thus difficult to achieve a good signal to noise ratio, despite an increase of the density of clusters, since the different transitions overlap in the whole energy range. Several structures lying very close in energy were found by ours and previous calculations.^{21,29,44,46,52,53} We find that two C_{2v} structures are the most stable geometries followed by C_s and C_{3v} structures. The large number of small intensity transitions results in a quasi continuous spectrum, which is difficult to compare with the measured one. Furthermore, because of the small energy separation, several isomers are expected to be present in the observed sample. Notice however the calculated s-type transitions below 3 eV, which can be correlated with the fine structure observed in the experimental spectrum.

V. DISCUSSION

Copper is one of the three coinage metals, its atomic ground state configuration ($Ar - 3d_{10}4s_1$) is similar to that of silver ($Kr - 4d_{10}5s_1$). A remarkable difference is, however, the energetic position of the d levels, which are approximately 2 eV below the s level in the case of copper but 4 eV in silver. In the limit of very large particles or bulk electronic structure, the s levels are extended to a large flat band and the d atomic states develop in a much more localized band. The frontier orbitals of this d band is approximately 4 eV below the Fermi energy in the case of silver, but only 2 eV in the case of copper. A similar situation occurs for small clusters. In the case of the dimers, we find that the HOMO-1 orbital which is predominantly of d-type is separated from the predominantly s-type HOMO orbital by 0.5 eV in the case of copper, while the separation amounts to 2.4 eV for the silver dimer. A similar situation occurs for the pentamers, we find that the separation between the d-type frontier orbital is separated from the s-type HOMO orbital by 1.9 eV in the case of copper, while it amounts to 3.3 eV for silver. This implies that transitions issued from d-type states appear at lower energies in the case of copper than for silver. The detailed situation depends on the particular clusters considered, but we find that typically (with

the exception of Cu_3 and Cu_4) the passage from s-type to d-s type transitions occurs in a range comprised between 2.5 and 3.0 eV in the case of copper and between 4.5 and 5.5 eV for silver clusters. Furthermore for copper aggregates there is a clear transition from d-s type to d-p type transitions around 5 eV, which can be seen as a dip in the oscillator strength in the theoretical spectra of Cu_3 and Cu_6 for example.

The experimental spectra of both silver and copper reflect these considerations. We find in silver^{16,33} that the experimental spectra are characterized by a small number of intense absorption lines situated below 4.5 eV and a more complex structure above 5 eV. The intense absorptions are in close agreement with the calculated s-type transitions and allow assigning given isomers to the measured spectra, while the higher energy d-type transitions are not well reproduced by the calculation. In the case of copper, the spectra are formed of a large number of lines, as an example the Cu_7 line spectrum must be decomposed into 34 different Gaussians in order to reproduce the experiment, while in the case of Ag_7 only ten different Gaussians are sufficient. This is clearly due to the large number of d-s or d-p transitions for copper clusters. If in some cases, as discussed in Sec. IV, the general behavior of the experimental spectrum is in relative agreement with the corresponding TD-DFT calculation, the detailed structure of the spectra is not reproduced. The situation is different for the low energy transitions marked by a dot in Fig. 2, which correspond to transitions issued from predominantly s-type orbitals. In this case there is a better correlation between the measured and calculated transitions as mentioned in the size by size analysis. This is in particular true for the C_{2v} and D_{5h} ground state configuration of, respectively, Cu_5 and Cu_7 . For Cu_6 and the closed shell Cu_8 cluster, the calculations predict intense s-s type transitions at low energy, they are in agreement with the experiment if we assume that the two lowest energy isomers contribute to the measured spectra for both Cu_6 and Cu_8 .

We conclude from this analysis that the complexity of the copper clusters experimental spectra is closely related to the emergence of d-type transitions at energies above 3 eV. The present TD-DFT calculation does not reproduce correctly the fine structure of the spectra above this limit. In the low energy range of the absorption, i.e., below 3.0 eV where s-s and s-p type transitions are dominant, the agreement between experiment and theory is better. From this point of view, the situation is similar to that observed for Ag clusters, the frontier energy being situated between 4.5 and 5.5 eV depending on the particular cluster considered.^{15,33} Idrobo *et al.*¹⁵ have made a detailed analysis of the effect of the d electrons on the optical absorption of silver clusters. They conclude that their primary effect is to quench the oscillatory strength by screening of the s electrons and second that they are involved in the optical transitions. Both effects intervene in the case of copper clusters, but as mentioned above the direct involvement of the d electrons in the optical transitions appears at lower energies in the case of copper and has a deeper influence on the optical absorption.

Figure 3 presents the experimental and theoretical values of the sum of the oscillator strengths per atom for the Cu_n ($n = 2-9$) clusters up to a cutoff energy of $E_{cut} = 5.5$ eV.

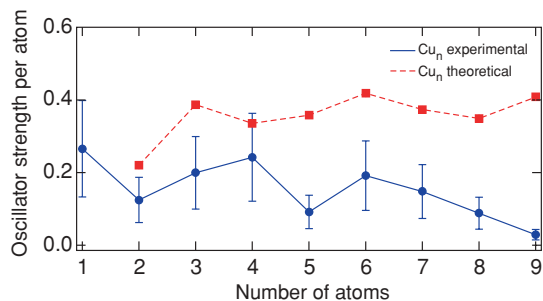


FIG. 3. Experimental and theoretical value of the oscillator strength per atom for Cu_n ($n = 1-9$) clusters integrated up to a photon energy of 5.5 eV. The theoretical value has been reported for the ground state configuration, except for the D_{2d} octamer. The systematic error of 50% on the measured absolute value is related to the uncertainty in determining the density of clusters per unit area.

Despite the uncertainty in the determination of the absolute experimental value, the average theoretical value is definitely larger than the experimental one. A similar situation occurs for gold clusters^{6,33} where the theoretical value exceeds by a factor of 2–5 the experimental one, the agreement is however better in the case of silver.³³ These measurements of OS suggest that, like in the case of the absorption, the TD-DFT scheme does not reproduce well the transitions in which a strong d component occurs.

Notice however that the effect of the matrix on the OS cannot be neglected. We find that the OS of the $^2P_{1/2,3/2} \leftarrow ^2S_{1/2}$ transition of Cu_1 in neon, equal to 0.26 with an uncertainty of 50%, does not agree with the corresponding gas phase value⁵⁴ equal to 0.65. A similar situation occurs in the case of gold.^{33,54} Such a difference between the gas phase and the matrix values has already been reported by Gruen *et al.*⁵⁵ They found that the OS of Au atoms in Ar, Kr, or Xe matrices decreases by a factor of 1.2, 1.8, and 2.5, respectively. For atomic silver the OS of the s-p transition,^{33,54} 0.72 and 0.71 in gas phase and in a neon matrix are in good agreement. This implies that the screening of the s electrons by the d electrons is modified by the presence of the matrix. This is also true for small clusters, which explains in part the discrepancy between experiment and theory.

VI. CONCLUSION

We have measured in the UV-visible range the absorption spectra of mass selected Cu_n ($n = 1-9$) clusters embedded in a solid neon matrix. They show a higher complexity and a larger number of transitions compared to similar sizes of silver clusters. Our measurements are compared to TD-DFT calculations implemented in the TURBOMOLE package, using the b3-lyp functional. These calculations indicate that for energies larger than 3 eV the transitions are of d-s and d-p type, while for Cu_5 , Cu_6 , Cu_7 , Cu_8 , and Cu_9 most of the transitions below 3 eV are issued from predominantly s states. The large number of d-type transitions correlates well with the complexity of the measured spectra; however, the TD-DFT scheme does not reproduce well the detailed structure of the absorption lines. We suggest that at energies lower than 3 eV, where in several cases s-s type transitions occur, the

correlation between experiment and theory is better. The sum of the oscillator strengths up to 5.5 eV for the different size clusters is reported, and shown to be on the average two to five times smaller than the calculated value. Comparison between experiment and theory suggests that the TD-DFT does not properly take into account the effect of the d electrons and that further calculations are necessary to understand in detail the nature of optical transitions in Cu clusters. In this sense these measurements may serve as benchmark to test the validity of different theoretical approaches.

ACKNOWLEDGMENTS

This work was supported by the Swiss National Science Foundation.

- V. Bonačić-Koutecký, P. Fantucci, and J. Koutecký, in *Metal Clusters*, edited by W. Ekaradt (Wiley, New York, 1999).
- J.-O. Joswig, L. Tunturivuori, and R. Nieminen, *J. Chem. Phys.* **128**, 014707 (2008).
- M. Vollmer and U. Kreibig, *Optical Properties of Metal Clusters* (Springer, New York, 1994).
- G. Celep, E. Cottancin, J. Lermé, M. Pellarin, L. Arnaud, J. R. Huntzinger, J. L. Vialle, M. Broyer, B. Palpant, O. Boisron, and P. Mélinon, *Phys. Rev. B* **70**, 165409 (2004).
- S. Fedrigo, W. Harbich, and J. Buttet, *Phys. Rev. B* **47**, 10706 (1993).
- S. Lecoultre, Ph.D. thesis, EPFL, 2009.
- D. M. Lindsay, F. Meyer, and W. Harbich, *Z. Phys. D* **12**, 1 (1989).
- F. Conus, J. T. Lau, V. Rodrigues, and C. Félix, *Rev. Sci. Instrum.* **77**, 113103 (2006).
- D. Kolb, H. Rotermund, W. Schrittenlacher, and W. Schroeder, *J. Chem. Phys.* **80**, 695 (1984).
- H. Wiggenhauser, D. Kolb, H. Rotermund, W. Schrittenlacher, and W. Schroeder, *Chem. Phys. Lett.* **122**, 71 (1985).
- M. Moskovits and J. E. Hulse, *J. Chem. Phys.* **67**, 4271 (1977).
- G. A. Ozin and S. A. Mitchell, *J. Phys. Chem.* **86**, 473 (1982).
- G. A. Ozin, S. A. Mitchell, D. F. McIntosh, S. M. Mattar, and J. Garcia-Prieto, *J. Phys. Chem.* **87**, 4651 (1983).
- J. Hormes, R. Grinter, B. Breithaupt, and D. Kolb, *J. Chem. Phys.* **78**, 158 (1983).
- J. C. Idrobo, S. Ögüt, and J. Jellinek, *Phys. Rev. B* **72**, 085445 (2005).
- M. Harb, F. Rabilloud, D. Simon, A. Rydlo, S. Lecoultre, F. Conus, V. Rodrigues, and C. Félix, *J. Chem. Phys.* **129**, 194108 (2008).
- M. Tiago, J. Idrobo, S. Ogut, J. Jellinek, and J. Chelikowsky, *Phys. Rev. B* **79**, 155419 (2009).
- S. Ogut, J. Idrobo, J. Jellinek, and J. Wang, *J. Cluster Sci.* **17**, 609 (2006).
- J. C. Idrobo, W. Walkosz, S. F. Yip, S. Ogut, J. Wang, and J. Jellinek, *Phys. Rev. B* **76**, 205422 (2007).
- S. Fedrigo, W. Harbich, and J. Buttet, *Phys. Rev. B* **58**, 7428 (1998).
- M. Yang, K. A. Jackson, C. Koehler, T. Frauenheim, and J. Jellinek, *J. Chem. Phys.* **124**, 1 (2006).
- X. Wang, X. Wan, H. Zhou, S. Takami, M. Kubo, and A. Miyamoto, *J. Mol. Struct.* **579**, 221 (2002).
- S. P. Walch and B. C. Laskowski, *J. Chem. Phys.* **84**, 2734 (1986).
- E. Miyoshi, H. Tatewaki, and T. Nakamura, *J. Chem. Phys.* **78**, 815 (1983).
- A. Becke, *Phys. Rev. A* **38**, 3098 (1988).
- C. Lee, W. Yang, and R. Parr, *Phys. Rev. B* **37**, 785 (1988).
- F. Weigend and R. Ahlrichs, *Phys. Chem. Chem. Phys.* **7**, 3297 (2005).
- O. Treutler and R. Ahlrichs, *J. Chem. Phys.* **102**, 346 (1995).
- E. M. Fernández, J. M. Soler, I. L. Garzon, and L. C. Balbas, *Phys. Rev. B* **70**, 165403 (2004).
- R. Bauernschmitt and R. Ahlrichs, *Chem. Phys. Lett.* **256**, 454 (1996).
- R. Ahlrichs, M. Bar, M. Haser, H. Horn, and C. Kolmel, *Chem. Phys. Lett.* **162**, 165 (1989).
- W. Begemann, K. H. Meiwes Broer, and H. O. Lutz, *Phys. Rev. Lett.* **56**, 2248 (1986).
- S. Lecoultre, A. Rydlo, J. Buttet, C. Félix, S. Gilb, and W. Harbich, *J. Chem. Phys.* **134**, 074302 (2011).

- ³⁴C. Moore, *Atomic Energy Levels, Vol. II (Chromium through Niobium)* (U.S. Government Printing Office, Gaithersburg, 1952).
- ³⁵M. D. Morse, *Chem. Rev.* **86**, 1049 (1986).
- ³⁶M. Moskovits, *Chem. Phys. Lett.* **118**, 111 (1985).
- ³⁷D. P. DiLella, K. Taylor, and M. Moskovits, *J. Phys. Chem.* **87**, 524 (1983).
- ³⁸J. A. Howard, K. F. Preston, R. Sutcliffe, and B. Mile, *J. Phys. Chem.* **87**, 536 (1983).
- ³⁹M. Morse, J. Hopkins, P. Langridge-Smith, and R. Smalley, *J. Chem. Phys.* **79**, 5316 (1983).
- ⁴⁰M. Morse, *Chem. Rev.* **86**, 1049 (1986).
- ⁴¹M. Knickelbein, *J. Chem. Phys.* **100**, 4729 (1994).
- ⁴²A. Ramirez-Solis, O. Novaro, and M. E. Ruiz, *Phys. Rev. B* **35**, 4082 (1987).
- ⁴³C. Massobrio, A. Pasquarello, and R. Car, *Chem. Phys. Lett.* **238**, 215 (1995).
- ⁴⁴K. Jug, B. Zimmermann, P. Calaminici, and A. M. Koster, *J. Chem. Phys.* **116**, 4497 (2002).
- ⁴⁵P. Calaminici, A. M. Köster, N. Russo, and D. R. Salahub, *J. Chem. Phys.* **105**, 9546 (1996).
- ⁴⁶P. Jaque and A. Toro-Labbé, *J. Chem. Phys.* **117**, 3208 (2002).
- ⁴⁷Y. Shen and J. J. BelBruno, *J. Phys. Chem.* **109**, 512 (2005).
- ⁴⁸K. Balasubramanian and P. Feng, *J. Phys. Chem.* **94**, 1536 (1990).
- ⁴⁹C. W. Bauschlicher, S. R. Langhoff, and H. Partridge, *J. Chem. Phys.* **93**, 8133 (1990).
- ⁵⁰K. A. Jackson, *Phys. Rev. B* **47**, 9715 (1993).
- ⁵¹C. Massobrio, A. Pasquarello, and A. Dal Corso, *J. Chem. Phys.* **109**, 6626 (1998).
- ⁵²M. Itoh, V. Kimar, and Y. Kawazoe, *Int. J. Mod. Phys. B* **19**, 2421 (2005).
- ⁵³G. H. Guvelioglu, P. Ma, X. He, R. C. Forrey, and H. Cheng, *Phys. Rev. Lett.* **94**, 026103 (2005).
- ⁵⁴J. Sansonetti, *Handbook of Basic Atomic Spectroscopic Data* (National Institute of Standards and Technology, Gaithersburg, 2010).
- ⁵⁵D. M. Gruen, S. L. Gaudioso, R. L. McBeth, and J. L. Lerner, *J. Chem. Phys.* **60**, 89 (1974).